A Numerical Study into the Dynamic Behaviour of a GPS Dropwindsonde in a Prescribed Wind Field

Sunwei, Li * and Craig A., Miller

Boudnary Layer Wind Tunnel Laboratory, University of Western Onatrio, London, ON

ABSTRACT

The GPS dropsonde has now been in use for over a decade, providing measurements of atmospheric variables, like wind velocities, air temperatures and humidity, with unprecedented resolution and accuracy in hurricanes. However, since the measurements are performed in neither a conventional Eulerian framework nor a perfect Lagrangian framework, it is not thoroughly understood as to how those measurements interpreted in terms of deriving mean profiles, turbulence profiles and wind spectra.

In this study, a numerical model is presented to simulate the fall of the GPS dropsonde through a wind field with prescribed mean and turbulence statistical characteristics. The falling dropsondes are tracked and then the wind field are extracted using the wind finding equation of Hock and Franklin (1999). The measured mean and turbulence profiles are compared with the prescribed values. Results show the wind finding equation gives a satisfactory agreement between the measured mean profiles with the prescribed ones. The measured turbulence profiles, on the other hand, exhibit more appreciable variations from the prescribed values when the same size of dataset, as in the mean profile comparison, is employed for composition. In addition, sensitivity analysis of post processing techniques, such as differentiation schemes used to calculated dropwindsonde acceleration and filter characteristics, is also conducted. The analysis shows although these techniques have little influence on the mean profile interpretation, it does impact the turbulence interpretation considerably. Wind spectra comparisons based on a spectral tensor model are also presented in this study. The comparison provided the evidence of that the GPS dropwindsonde measurements are capable of reproducing wind spectrum correctly along its trajectory given a proper spectral model is adopted for post processing.

1. Introduction

The direct measurement of wind velocities within the boundary layer region of tropical cyclones is distinguished, understandably, to be difficult. The GPS dropwindsonde provided the best chance, so far, of directly measuring wind velocities and other atmospheric variables in that region. Described by Hock and Franklin (1999), the GPS dropwindsonde can measure wind every half second with an accuracy in the order of $1m/s$ when it falls through the atmosphere. In the same study, they provided a wind finding equation, which extracts wind velocities from dropwindsonde measurements. Adopting this interpretation, many researchers (Kepert (2001); Kepert and Wang (2001); Powell et al. (2003); Vickery et al. (2009)) using GPS dropwindsonde data have advanced our understanding of the tropical cyclone wind structure, especially the vertical profiles in between of safe reconnaissance flight heights and sea surface which is hardly covered by other measurements.

Despite its wide use, the wind finding equation introduced by Hock and Franklin (1999) is derived from a linearization of the governing equations of the motion of the GPS dropwindsonde under certain assumptions which have not been thoroughly investigated. The purpose of this study is trying to examine the applicability of this equation by simulating the fall of dropwindsondes through a wind field with known statistical characteristics and then comparing the resulting simulated measurements with the known statistics to evaluate the validity of the GPS dropwindsonde measurements and to help interpret them.

Previous researches done on motion of falling, or rising objects, through the atmosphere serve as a start point for this study. Fichtl (1971) derived a set of coupled differential equations describing the motion of a rising, or falling, wind sensor under horizontal wind perturbations. Followed that analysis, Nastrom and Vanzandt (1982) investigated rising objects in the atmosphere by seeking an analytical solution to the governing equations of the motion of a sphere, including nonlinear responses. The differential equations introduced in their study forms the basis of deriving governing equations of the motion of the GPS dropwindsonde, which is the key in the numerical simulation used in this study.

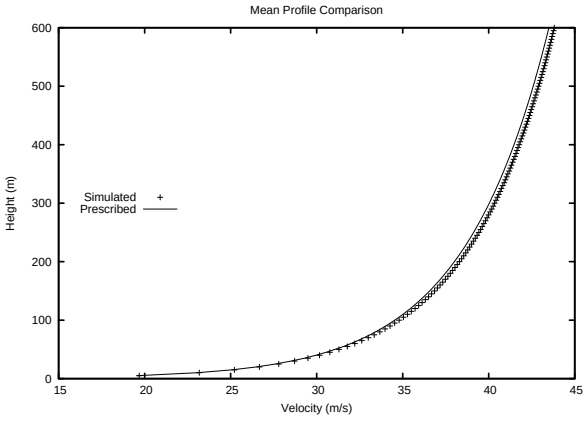

FIG. 1. Mean Velocity Profile Comparison, where prescribed means prescribed value while simulate means mean profile sampled from simulated wind field

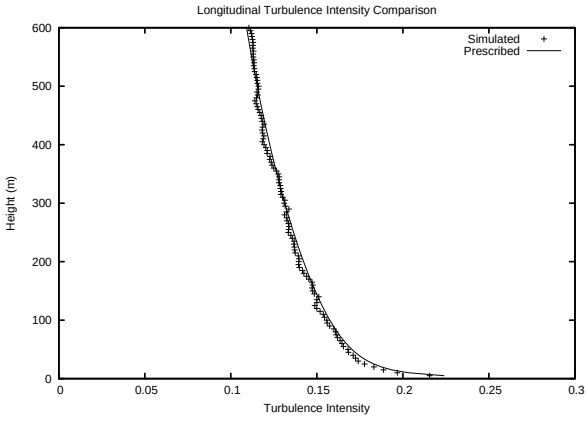

FIG. 2. Turbulent Intensity (Longitudinal Component) Profile Comparison, where prescribed means prescribed value while simulated means profile sampled from simulated wind filed

Wind fields with known statistical characteristics are generated using the spectral transformation techniques described by Solari et al. (2007) and Carassale et al. (2007). The statistical characteristics prescribed are mainly spectral representations following Hu (2007); Solari and Piccardo (2001), which are wind spectra, spatial correlations and point correlations. These spectral information are organized as spectrum matrix. Although this model is well validated by field experiments and engineering measurements (Solari and Piccardo 2001), it describes wind spatial relationships separately for longitudinal and vertical direction as wind spectra and spatial correlations. Thus, there is no explicit expression of spectrum when wind velocities are sampled vertically like the GPS dropwindsonde does. Thus, in addition to generating wind field using this spectrum matrix model, the spectral tensor model of Mann (1994) was also adopted which expresses wind spatial relationships in wave number space. Thus, from stand point of view of spectral tensor, there is no difference whether wind velocities are sampled in longitudinal direction or vertical direction in deriving wind spectrum. This gives the opportunity to use dropwindsonde measurements to explore the spectra of the wind field it falling through.

After this introduction,the wind field generation and validation will be discussed in section 2 while details of the simulation of the motion of a GPS dropwindsode through the simulated wind fields are given in section 3. Results from the simulated measurements are summarized and discussed in section 4. Conclusions and remarks for future research will be given in section 5.

2. Wind Field Generation

Both the wind field generation methods using the spectrum matrix model of Solari et al. (2007) and Carassale et al. (2007) and the spectral tensor model of Mann (1994) are discussed in detail in this section. The spectrum matrix modelled wind fields give reliable mean and turbulence profiles while the spectral tensor modelled wind fields are advantageous in describing wind spectrum in three spatial directions.

a. Spectrum matrix model

A spectrum matrix is capable of describing all the second order statistical characteristics of the simulated wind field, including all wind spectra, spatial cross spectra and point cross spectra. After the spectrum matrix is specified, DFT (Discrete Fourier Transformation) can be employed to transform these spectral representations into a stochastic wind field.

In this study, the spectrum matrix uses wind spectra model described by Von Karman (1948), while spatial correlations are governed by exponential decay function of Solari and Piccardo (2001) which is an extension of model provided by Davenport (1967) and the point correlations given by Solari and Piccardo (2001).

To simplify the discussion, only the one-dimensional, vertical wind field is generated here. The wind field is discretized into 120 points vertically, spaced at $5m$ intervals, while the simulated time history uses a time step of 0.1 seconds for a total time of 6553.6 seconds.

The simulation is validated by comparing statistical characteristics of the simulated wind field with prescribed parameters. The comparison shows that wind fields simulated are good stochastic realization of prescribed statistics. Figure.1 shows the mean profile comparison of the log-law governed wind field. Figure.2 and Figure.3 show comparisons of the logitudinal turbulence intensity and tur-

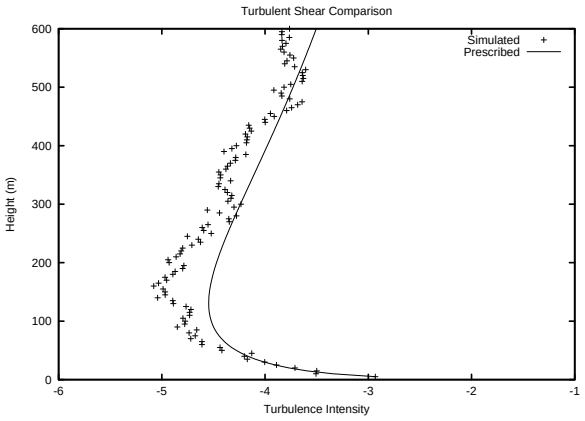

FIG. 3. Turbulent Shear (UW Shear) Profile Comparison, where prescribed means prescribed value while simulated means profile sampled from simulated wind field

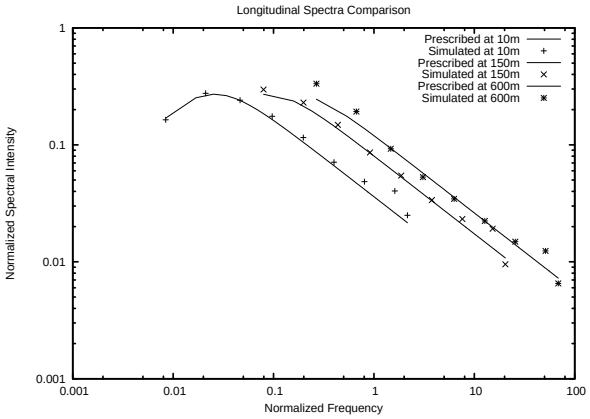

FIG. 4. Spectral Density Comparison for longitudinal wind, where prescribed means prescribed value while simulated means spectrum measured from simulated wind field

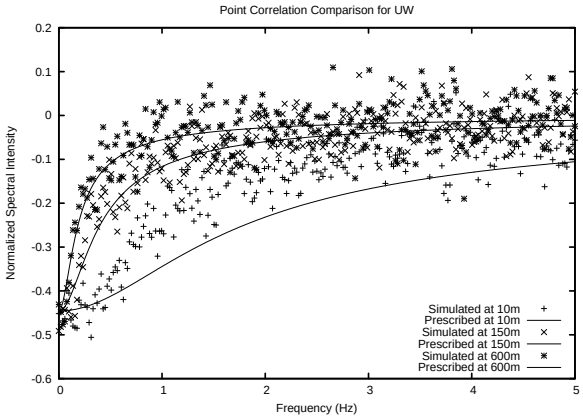

FIG. 5. Cross Spectral Density Comparison for longitudinal wind and vertical wind, where prescribed means prescribed value while simulated means spectrum measured from simulated wind field

bulent shear stress for the same wind field. The spectra validation is covered by Figs.4 and 5, which show the longitudinal wind spectrum comparison and the point correlation for longitudinal and vertical wind comparison respectively.

b. Spectral tensor model

In addition to spectrum matrix model described above, a wind field simulated following Mann (1998) is utilized in this study to explore the possibility of extracting spectral information from the GPS dropwindsonde measurements. Unlike the spectrum matrix model, the spectral tensor model depicts the three-dimensional wind field in terms of a tensor formulated in wave number space. Thus, sampling the wind in the vertical direction is not different from sampling it in the along-wind direction as it is in the conventional way. So, wind velocities measured by the GPS dropwindsonde when it falls through the atmosphere can be used to derive the conventional longitudinal wind spectrum.

Both the wind tensor model and the simulation techniques are described by Mann (1998). A more comprehensive study on the spectral tensor is provided by Mann (1994). Slightly different from the wind field generated using the spectrum matrix model, the wind field simulated using the spectral tensor model is two dimensional with no time history. Thus, Taylor's hypothesis (Mann 1998) is invoked to find wind at a discrete point at a discrete time. 128 points in vertical axis while 65536 points in longitudinal axis are utilized. Giving the longitudinal step and vertical step are 0.1 meters and 4.6875 meters, the total length in this simulation is $6553.5m$ while the total height remains the same as in the spectrum matrix case, which is $600m$.

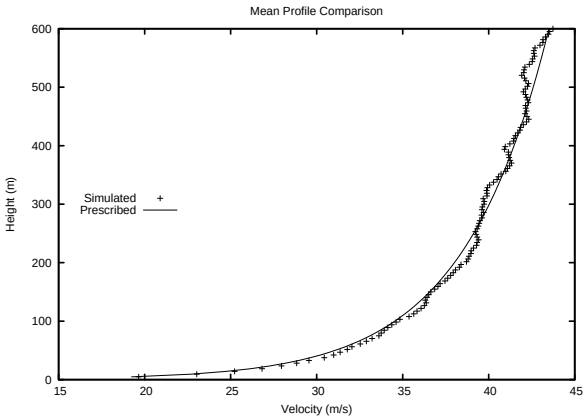

FIG. 6. Mean Velocity Profile Comparison, where prescribed means prescribed value while simulate means mean profile sampled from simulated wind field

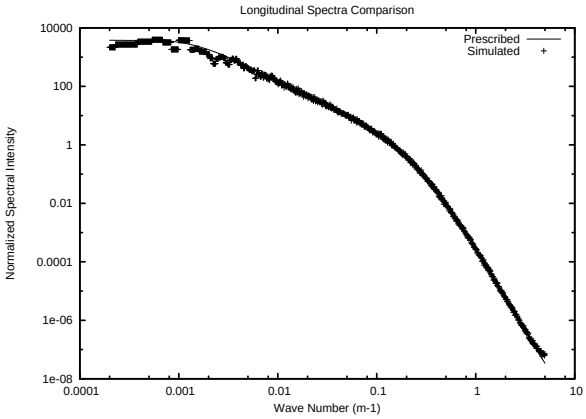

FIG. 7. Spectral Density Comparison for longitudinal wind, where prescribed means prescribed value while simulated means spectrum measured from simulated wind field

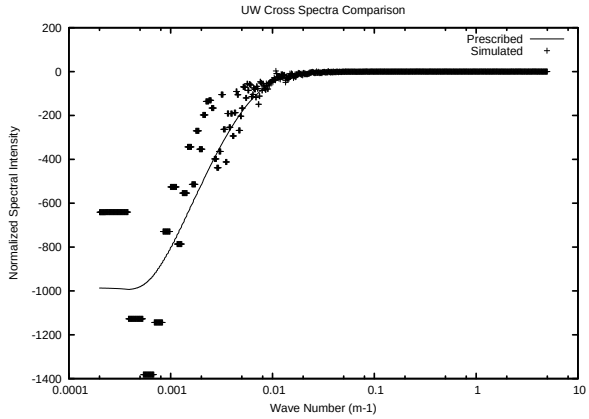

FIG. 8. Cross Spectral Density Comparison for longitudinal wind and vertical wind, where prescribed means prescribed value while simulated means spectrum measured from simulated wind field

Unlike validation in the spectrum matrix case, validation in the spectral tensor model case concentrates on the spectral representation of the wind field since we are interested in exploring the possibility of extracting spectral information from the GPS dropwindsonde measurements. Figure.6 shows the comparison of the mean profile in the log-law governed wind field. Figs.7 and 8 show comparisons of the spectrum of longitudinal wind and the cross spectrum of longitudinal and vertical wind.

3. Simulation of motion of GPS dropwindsonde

When the GPS dropwindsode is viewed as a point with certain mass falling through the atmosphere, the governing equations of its motion are similar to ones derived by Fichtl (1971). Since they are the equations governing a nonlinear system with three DOF (Degree of Freedom), some numerical integration methods should be used to solve it.

Moreover, raw measurements made by the GPS dropwindsonde need to be filtered to get rid of noises buried in its signal. Also, measured dropwindsode velocities need to be differentiated to get accelerations if wind finding equation introduced by Hock and Franklin (1999) is used to interpret the measurements.Thus, this simulation of the dropwindsonde motion gives an opportunity to evaluate the influence of those post processing techniques on the final interpretation.

a. Governing equations of motion of a GPS dropwindsonde

Motion of GPS dropwindsonde in the atmospheric boundary layer wind field is essentially the dynamic response of a nonlinear system under the stochastic external excitation. Hock and Franklin (1999) provided a brief discussion in an

appendix on the governing equations of the motion of the GPS dropwindsonde before generating a linearized version under several explicit assumptions. Different from focusing on the simplification of the governing equation,Nastrom and Vanzandt (1982) conduct a more comprehensive analytical analysis on rising objects in the atmosphere which includes discussions on a set of similar equations with full nonlinearity.

Simply just summarized and extended studies mentioned above, the governing equations of the motion of the GPS dropwindsondes will be presented here. When dropwindsondes fall through the atmosphere, the drag generated by interaction between parachute of the dropwindsonde and the wind can be modeled as

$$\begin{aligned} F_{Dx} &= \frac{1}{2}\rho A C_D \frac{u-\dot{x}}{\sqrt{(u-\dot{x})^2+(v-\dot{y})^2+(w-\dot{z})^2}} \\ F_{Dy} &= \frac{1}{2}\rho A C_D \frac{v-\dot{y}}{\sqrt{(u-\dot{x})^2+(v-\dot{y})^2+(w-\dot{z})^2}} \\ F_{Dz} &= \frac{1}{2}\rho A C_D \frac{w-\dot{z}}{\sqrt{(u-\dot{x})^2+(v-\dot{y})^2+(w-\dot{z})^2}} \end{aligned} \quad (1)$$

where F is the force in which the subscript stands for the direction, C_D is the drag coefficient of the system contributed mainly by parachute, A gives the cross section area, and ρ gives the density of air, assuming to be constant in simulated falls. If (x, y, z), as a vector, is used to give the position of the GPS dropwinsonde, $(\dot{x}, \dot{y}, \dot{z})$ indicates the the velocity of the dropwindsonde at position (x, y, z). Similarly, (u, v, w) is employed as the wind velocity vector. Since the gravity and drag forces are only forces that the dropwindsonde experiences when it falls, the motion of the dropwindsonde can be determined by combining of these two types of forces as

$$\begin{aligned} m\ddot{x} &= \frac{1}{2}\rho A C_D \frac{u-\dot{x}}{\sqrt{(u-\dot{x})^2+(v-\dot{y})^2+(w-\dot{z})^2}} \\ m\ddot{y} &= \frac{1}{2}\rho A C_D \frac{v-\dot{y}}{\sqrt{(u-\dot{x})^2+(v-\dot{y})^2+(w-\dot{z})^2}} \\ m\ddot{z} &= \frac{1}{2}\rho A C_D \frac{w-\dot{z}}{\sqrt{(u-\dot{x})^2+(v-\dot{y})^2+(w-\dot{z})^2}} - mg \end{aligned} \quad (2)$$

where $(\ddot{x}, \ddot{y}, \ddot{z})$ indicates the acceleration of the dropwindsonde and m is the mass of the dropwindsonde system.

Equation (2) is a set of coupled nonlinear ODEs (Ordinary Differential Equation) governing the motion of the dropwindsonde. Thus, it is extremely difficult, if it is not impossible, to solve analytically, and some numerical integration techniques are required to give a discrete solution. In this case we use the fourth order Runge-Kutta method, described by Chapra and Canale (2010) to numerically integrate the equations. The numerical solution, velocity of the dropwindsonde, to equation (2), is sought along the trajectory of the dropwindsonde and then position of dropwindsonde is found by integrating the solution while acceleration is obtained by differentiating it.

b. Post processing of GPS dropwindsonde measurements

When GPS dropwindsonde measurements were used, post processing is conducted to, firstly get rid of the noise in its signal and secondly to add a correction term to extract the wind velocities from the raw measurements. According to Hock and Franklin (1999), the correction term includes the acceleration and the falling rate of the dropwindsonde. Since there is no direct measurements of the acceleration, these values are typically obtained by differentiating the velocities and the static pressure measured by the dropwindsonde. Thus, to evaluate influence of different post processing techniques, both differentiation schemes used to calculated the acceleration terms and low-pass filter characteristics are investigated.

Only briefly mentioned in (Franklin et al. 2003; Vickery et al. 2009), low-pass filters did not receive a detailed discussion. Therefore, only commonly used filters will be investigated. In other words, both the first order and second order Butterworth filter and the moving average method, acting as a low-pass filter, will be evaluated. Another factor associated with the filter is the cut-off frequency. Mentioned by Franklin et al. (2003), low-pass filter with cut-off time scale of $3s$ is applied to post process the GPS dropsonde measurements in their study. Therefore, $2s$, $3s$, $4s$ are, as filter cut-off scales, investigated in this study.

As to differentiation schemes, since the first order backward differentiation is widely used in interpreting dropwindsonde measurements, it is included in this sensitivity analysis. Because higher order differentiation usually gives more accurate results, differentiation schemes of second and third order are also evaluated. Thus, in this study, first and second order of both forward and backward differentiation, together with second and third order of central differentiation, are used to post process dropwindsonde measurements and then final results are compared.

4. Results and Discussion

Comparisons of results coming from the dropwindsonde simulation, after post processing described by section b, and prescribed statistical characteristics of simulated wind fields are shown in following figures. The comparison and discussion will be divided according to the models used to generate the wind field. Results from the spectrum matrix modelled wind field will be mainly used to examine mean and turbulence profiles while results from the spectral tensor modelled wind fields will be used to explore the possibility of extracting spectral information from the GPS dropwindsonde measurements.

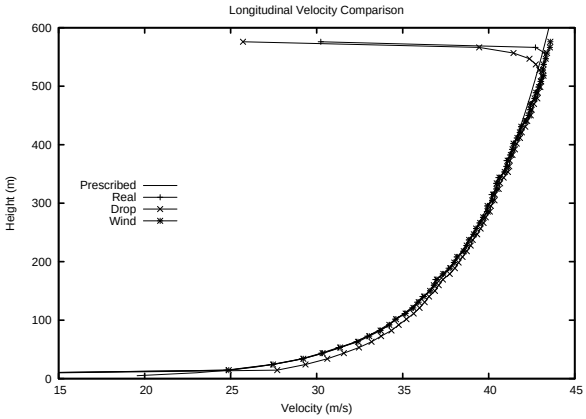

FIG. 9. Mean Velocity Profile Comparison, where prescribed means prescribed value associated with generated wind field, Real means velocity calculated using wind finding equation with true acceleration, drop means velocity of dropwindsonde along while wind means local wind extracted from wind field at the moment dropwindsonde passed by

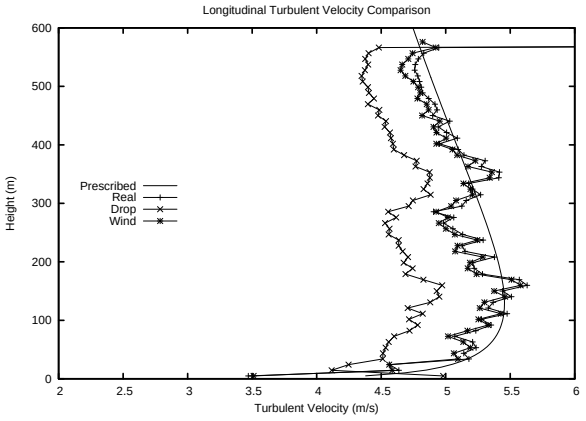

FIG. 10. Turbulent Velocity Profile Comparison, where prescribed means prescribed value associated with generated wind field, Real means turbulence calculated using wind finding equation with true acceleration, drop means turbulent velocity of dropwindsonde along while wind means turbulent local wind extracted from wind field at the moment dropwindsonde passed by

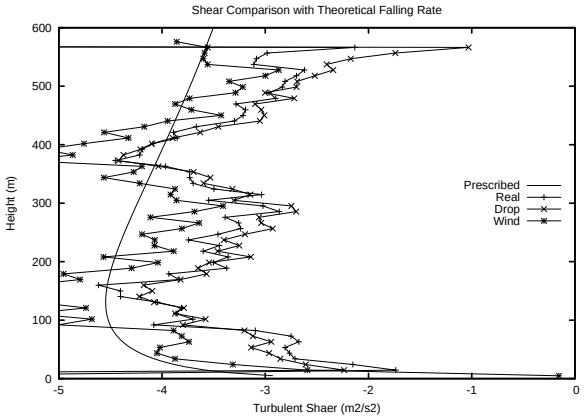

FIG. 11. Turbulent Shear Profile Comparison, where prescribed means prescribed value associated with generated wind field, Real means shear calculated with wind finding equation derived horizontal wind, drop means shear calculated with horizontal wind measured directly by dropwindsonde while wind means local wind shear extracted from wind field at the moment dropwindsonde passed by

a. Spectrum Matrix Modelled Wind

Figure.9 shows mean profiles comparison in case of log-law governed wind field. The very good agreement substantiates the use of the wind finding equation introduced by Hock and Franklin (1999) in mean wind profile interpretation. Although there is appreciable difference between dropwindsonde velocities and real wind velocities in the lowest portion of the wind field, the acceleration correction term in the wind finding equation removes much of this difference. On the other hand, the rms velocity fluctuation and turbulent shear comparisons, shown in Fig.10 and Fig. 11, do not share the same satisfactory level of agreement as in the mean profile comparison. As shown in these figures, the dropwindsonde has the ability to capture the general shape of the variation of the turbulence along its path, although the measured quantities deviate from the prescribed values randomly by considerable amounts when compared to the mean profile case.

Figures.12 and 13 shown that when mean profile is of interest, the use of different post processing techniques, such as different filters, different filter scales and different differentiation schemes, have no significant impact on the final mean profile produced. However, their influence is pronounced when turbulence information is of interest. As shown in Fig.14 and 15, both differentiation schemes and filters characteristics have the an appreciable impact on the post processed turbulent velocity profile. In Fig.15, different differentiation schemes used to derive acceleration of dropwinsonde are compared. Although higher order central differentiation gives rms velocity fluctuation profile closer

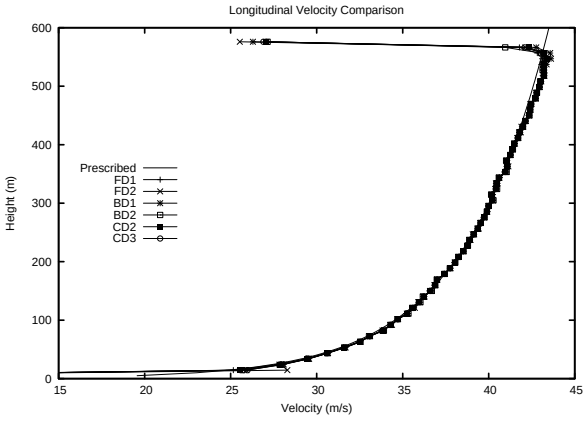

FIG. 12. Mean Velocity Profile Comparison when different differentiation schemes are employed, where FD1 stands for 1^{st} order forward differentiation, FD2 stands for 2^{nd} order forward differentiation, BD1 stands for 1^{st} order backward differentiation,BD2 stands for 2^{nd} order backward differentiation, CD2 stands for 2^{nd} order central differentiation and CD3 stands for 3^{rd} order central differentiation

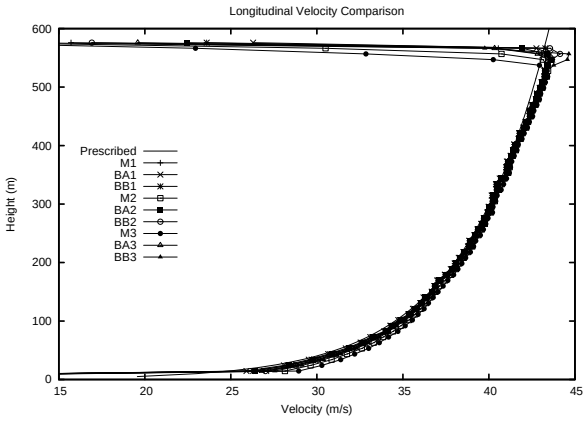

FIG. 13. Mean Velocity Profile Comparison when different filter characters are employed, M1 stands for moving average with 2s filter scale, M2 stands for moving average with 3s filter, M3 stands for moving average with 4s filter scale, BA1 stands for 1^{st} order Butterworth filter with 2s filter scale, BA2 stands for 1^{st} order Butterworth filter with 3s filter scale, BA3 stands for 1^{st} order Butterworth filter with 4s filter scale, BB1 stands for 2^{nd} order Butterworth filter with filter scale 2s, BB2 stands for 2^{nd} order Butterworth filter with filter scale 3s, BB3 stands for 2^{nd} order Butterworth filter with filter scale 4s

to prescribed profile than lower order differentiation, there is no significant improvement shown. Additionally, first order backward differentiation, which is commonly used in calculating acceleration term in practise, share the same level of accuracy as high order differentiation while second order backward differentiation overestimate the turbulence. Compared with differentiation schemes, different filter characteristics have a greater impact. As shown in Fig.14, moving average always underestimates the turbulence regardless of what filter scale is used. By comparison, Butterworth Filter is better in predicting rms velocity fluctuation. The scale of filter, or cut-off frequency, by far overweights the order of filter in terms of influence when the Butterworth filter is used. This can be seen in the Fig. 14 that difference between profiles interpreted using different filter scale is obviously larger than difference coming from the use of different order of Butterworth filter.

Another factor has been investigated in this study is the size of the dataset to be composited to get statistical meaningful results. As shown in Fig.16, mean profiles measured by the GPS dropwindsonde converged to the prescribed value when size of dataset used to composite exceeded 500, as the difference between composited profile and the prescribed value being of the order of $0.1m/s$. However, turbulence information needs a larger size of dataset to get a statistically converged profile. Like showing in Fig.17, rms velocity profile composited of 500 individual profiles still exhibits random variation large enough to bury prescribed shape. Thus, Fig.17 suggests a larger dataset of individual profiles should be utilized if turbulence information is of

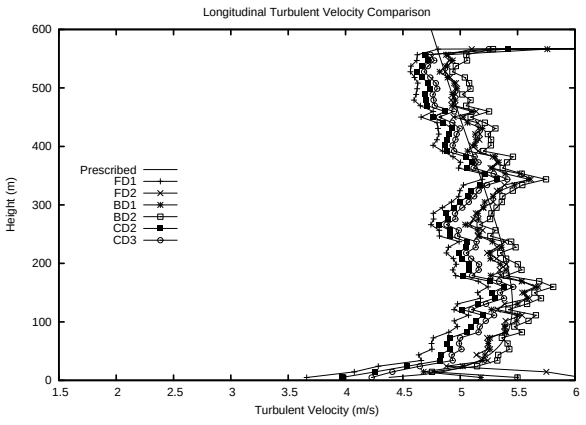

FIG. 14. Turbulent Velocity Profile Comparison when different differentiation schemes are employed, where FD1 stands for 1^{st} order forward differentiation, FD2 stands for 2^{nd} order forward differentiation, BD1 stands for 1^{st} order backward differentiation,BD2 stands for 2^{nd} order backward differentiation, CD2 stands for 2^{nd} order central differentiation and CD3 stands for 3^{rd} order central differentiation

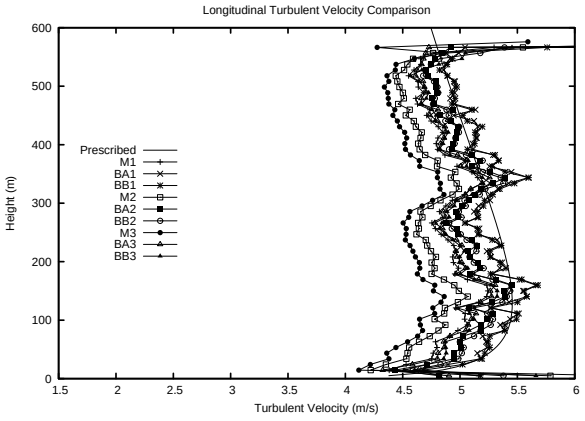

FIG. 15. Turbulent Velocity Profile Comparison when different filter characters are employed, M1 stands for moving average with 2s filter scale, M2 stands for moving average with 3s filter, M3 stands for moving average with 4s filter scale, BA1 stands for 1^{st} order Butterworth filter with 2s filter scale, BA2 stands for 1^{st} order Butterworth filter with 3s filter scale, BA3 stands for 1^{st} order Butterworth filter with 4s filter scale, BB1 stands for 2^{nd} order Butterworth filter with filter scale 2s, BB2 stands for 2^{nd} order Butterworth filter with filter scale 3s, BB3 stands for 2^{nd} order Butterworth filter with filter scale 4s

interest.

As for the rms velocity fluctuation profile comparison, the turbulent shear comparison shows the post processing techniques share the same impact on the final turbulent shear measured as in Fig.18 and Fig.19. However, the deviation of measured value from the prescribed ones are more appreciable in this case than in the case of rms velocity fluctuation profile comparison. Perhaps it is because the variation of the vertical wind velocity also contributes in this case. Naturally, this would leads to conclusion that even more data is needed to composite a statistical converged profile when turbulent shear is of interest, as shown in Fig.20.

b. Spectral Tensor Model

Simulation of the GPS dropwindsonde though the spectral tensor modelled wind field gives the opportunity to explore the possibility of extracting spectral information about wind field from the dropwindsonde measurements. Thus, the comparison in this part will focus on the spectrum extracted from the dropwindsonde measurements and the spectrum prescribed by the spectral tensor model.

The spectral tensor described wind field in terms of spectral density in wave number space in all three directions. Therefore, the spectral tensor model is capable of giving wind spectrum in any direction by integrating the

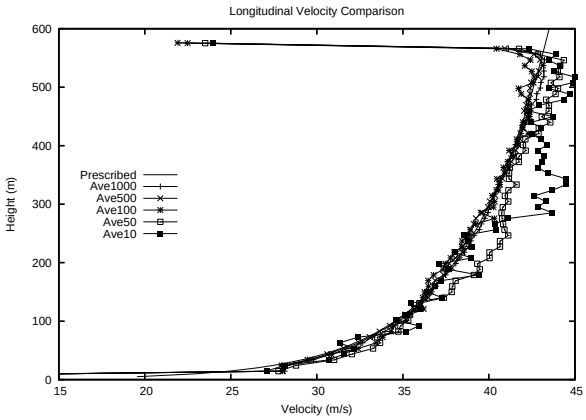

FIG. 16. Mean Velocity Profile Comparison with different composition data size, where number of composited data size indicated by key

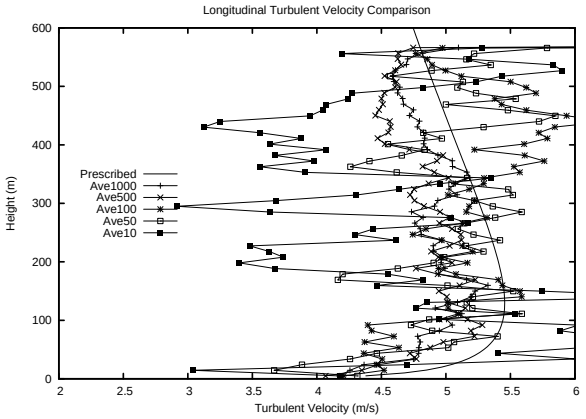

FIG. 17. Turbulent Velocity Profile Comparison with different composition data size, where number of composited data size indicated by key

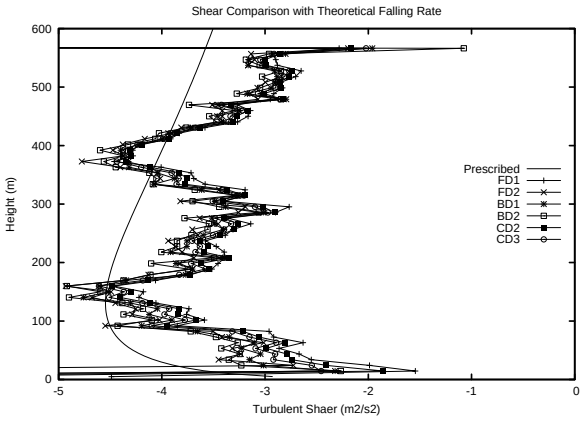

FIG. 18. Turbulent Shear Profile Comparison when different differentiation schemes are employed, where FD1 stands for 1^{st} order forward differentiation, FD2 stands for 2^{nd} order forward differentiation, BD1 stands for 1^{st} order backward differentiation,BD2 stands for 2^{nd} order backward differentiation, CD2 stands for 2^{nd} order central differentiation and CD3 stands for 3^{rd} order central differentiation

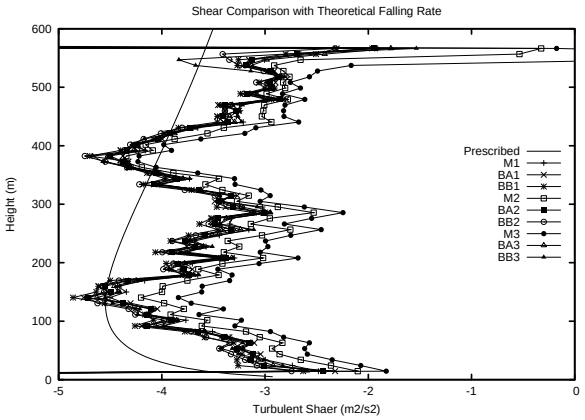

FIG. 19. Turbulent Shear Profile Comparison when different filter characters are employed, M1 stands for moving average with 2s filter scale, M2 stands for moving average with 3s filter, M3 stands for moving average with 4s filter scale, BA1 stands for 1^{st} order Butterworth filter with 2s filter scale, BA2 stands for 1^{st} order Butterworth filter with 3s filter scale, BA3 stands for 1^{st} order Butterworth filter with 4s filter scale, BB1 stands for 2^{nd} order Butterworth filter with filter scale 2s, BB2 stands for 2^{nd} order Butterworth filter with filter scale 3s, BB3 stands for 2^{nd} order Butterworth filter with filter scale 4s

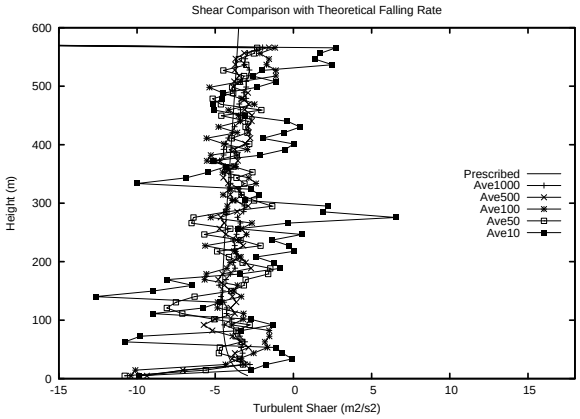

FIG. 20. Turbulent Shear Profile Comparison with different composition data size, where number of composited data size indicated by key

tensor along the other two directions perpendicular to the target direction. In other words, wind spectrum coming from the dropwindsonde measurements should be recovered by integrating the spectral tensor along k_1 and k_2 axis in wave number space which represent the along-wind and cross-wind direction in physical space.

A comparison between the prescribed and the measured longitudinal wind spectrum is shown in Fig.21, and also shows GPS dropwindsonde is capable of giving spectral information about the measured wind field. It is seen in the figure that the dropwindsonde can pick up spectral energy in the relative low wave number region where the predominant energy of the wind exists, except in the very low wave number region. The underestimation of spectral density in this region may be due to lack of measurements in this region rather than incapacity of the dropwindsonde measurements. In contrast, GSP dropwindsonde signal alone underestimates spectral density in the relative high wave number region. However, the acceleration term of the wind finding equation correct this underestimation.

Figure.22 shows a comparison for the cross spectra of the longitudinal and vertical components of wind. Similar to the comparison for the longitudinal spectrum, the GPS dropwindsonde is capable of reporting the general trend of the spectral density, and as before measured spectral density deviates from its prescribed value in the very low wave number region. As in the comparison of the longitudinal spectrum, the same explanation may also apply in this case.

5. Conclusion and Remark for Future Study

In this study, dropwindsondes are simulated to fall through wind fields with prescribed statistical characteristics. Two models describing spectral density of wind energy are adopted,

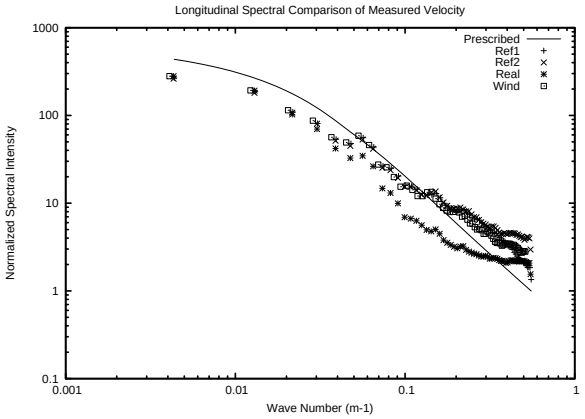

FIG. 21. Longitudinal Spectral Density Comparison, where prescribed refers to value integrated from spectral tensor, Ref1 refers to value post processed using 1^{st} order backward differentiation and 1^{st} order Butterworth filter with filter scale 3s, Ref2 refers to value post processed using true acceleration, Wind refers to local wind in wind field at moment when dropwindsonde passed by

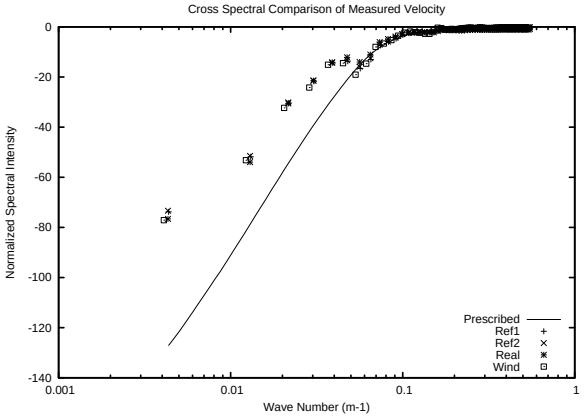

FIG. 22. where prescribed refers to value integrated from spectral tensor, Ref1 refers to value post processed using 1^{st} order backward differentiation and 1^{st} order Butterworth filter with filter scale 3s, Ref2 refers to value post processed using true acceleration, Wind refers to local wind in wind field at moment when dropwindsonde passed by

one is the spectrum matrix model while the other is the spectral tensor model. Validations of wind finding equation introduced by Hock and Franklin (1999) is conducted based on the motion simulation of the dropwindsonde. In addition to validations, simulations also give a sense of the impact of different post processing techniques, like filter types, filter scales and differentiation schemes, on the final interpretation of measurements. Other factors has been investigated are the size of dataset of composition to get statistical meaningful results and possibility to extract spectral information from the dropwindsonde measurements.

Comparison between statistics measured by the GPS dropwindsonde and its corresponding prescribed values indicates the GPS dropwindsonde is capable of reporting mean wind profiles with satisfactory accuracy. With help of the wind finding equation introduced by Hock and Franklin (1999), differences between the measured mean profiles and prescribed values can be removed in the region where mean profile rapidly changed with height. Although the GPS dropwindsonde measurements also captured the variation trends of turbulence profiles, agreements did not achieve the same level as in mean profiles comparison. However, although measured turbulence statistics deviated from its prescribed value appreciably, no systematical error is found, and the deviation reduced when composite data size increased, which means turbulence information can be extracted when the measurements are abundant.

Although no significant differences in the mean profiles comparison is found when different post processing techniques are employed, they do have considerable influence on turbulence statistics derived from the dropwindsonde measurements. Comparisons of rms velocity fluctuation profiles and turbulent shear profiles suggest that the filter characteristics are more influential when compared with differentiation schemes used to calculate the acceleration term. Although high order central differentiation schemes give velocity fluctuation profiles slightly closer than lower order schemes, no significant improvement is shown. Comparing with Butterworth filter, moving average perform poorly by underestimating turbulence. Filter scale, or cut-off frequency, is more influential when compared with filter order as Butterworth filter is used.

Understandably, composition data size has impact on credibility and variation of final interpretation of dropwindsonde measurements. Composited mean profile is stable when size of dataset of individual profiles exceed 500 while compositing turbulence profile needs a larger dataset to get statistically meaningful results.

To explore the possibility of extracting spectral information about wind field from the GPS dropwindsonde measurements, the simulation of dropwindsondes falling through the spectral tensor modelled wind field is analyzed. Comparison of the measured wind spectrum with the prescribed wind spectrum suggests the dropwindsonde is able to pick

up most significant spectral energy. However, the dropwindsonde velocity alone underestimate spectral density in energy containing wave number region while acceleration corrections give this missing energy back.

With help of this study, both mean profiles and turbulence informations can be extracted from the dropwindsonde measurements available. The wind finding equation, validated by this numerical simulation, is good interpretation in terms of not only mean profiles but also turbulence information, although care needs to be taken when acceleration terms is calculated in deriving turbulence profiles. In addition to profiles, wind spectra can also be extracted from the dropwindsonde measurements. If the turbulence, as one significant factor in determining the energy and momentum exchange in hurricane, can be made clear by examining the dropwindsonde measurements, our understanding of the hurricane wind structure and therefore the hurricane intensity prediction will be improved.

REFERENCES

Carassale, L., G. Solari, and F. Tubino, 2007: Proper orthogonal decomposition in wind engineering. part 2: Theoretical aspects and some applications. *Wind and Structure*, **10**, 177–208.

Chapra, S. C. and R. P. Canale, 2010: *Numerical Methods for Engineers*. McGraw-Hill Higher Education, 968 pp.

Davenport, A. G., 1967: The dependence of wind loads on meteorological parameters. *International Research Seminar on Wind Effects on Buildings and Structures*, Ottawa,ON,Canada, National Research Council of Canada, 19–82.

Fichtl, G. H., 1971: The responses of rising or falling spherical wind sensor to atmospheric wind perturbations. *J. Appl. Meteor.*, **10**, 1275–1284.

Franklin, J. L., M. L. Black, and V. K., 2003: Gps dropwindsonde wind profiles in hurricanes and their operational implications. *Wea. Forecasting*, **18**, 32–44.

Hock, T. F. and J. L. Franklin, 1999: The NCAR GSP dropwindsonde. *Bull. Amer. Meteor. Soc.*, **80**, 407–420.

Hu, L., 2007: Simulation of Stochastic Wind fields on Long-Span Bridges Based on Proper Orthogonal Decomposition. Ph.D. thesis, Huazhong University of Science & Technology, Wuhan, China, 189 pp., [Poersonal Communication].

Kepert, J., 2001: The dynamic of boundary layer jet with in tropical cyclone, part i: linear theory. *J. Atmos. Sci.*, **58**, 2469–2484.

Kepert, J. and Y. Wang, 2001: The dynamic of boundary layer jet with in tropical cyclone, part ii: nonlinear enhancement. *J. Atmos. Sci.*, **58**, 2485–2501.

Mann, J., 1994: The spatial structure of neutral atmospheric surface-layer turbulence. *J. Fluid Mech.*, **273**, 141–168.

Mann, J., 1998: Wind field simulation. *Prob. Eng. Mech.*, **13**, 269–282.

Nastrom, G. D. and T. E. Vanzandt, 1982: An analytical study of nonlinear response of rising balloons to horizontal wind. *J. Appl. Meteor.*, **21**, 413–419.

Powell, M. D., P. J. Vickery, and T. A. Reinhold, 2003: Reduced drag coefficient for high wind speed in tropical cyclone. *Nature*, **422**, 279–283.

Solari, G., L. Carassale, and F. Tubino, 2007: Proper orthogonal decomposition in wind engineering. part 1: A state-of-the-art and some prospects. *Wind and Structure*, **10**, 153–176.

Solari, G. and G. Piccardo, 2001: 3-d turbulence modeling for gust buffeting of structures. *Prob. Eng. Mech.*, **16**, 73–86.

Vickery, P. J., D. Wadhera, M. D. Powell, and Y. Chen, 2009: A hurricane boundary layer and wind field model for use in engineering application. *J. Appl. Meteor. Climatol.*, **48**, 381–405.

Von Karman, T., 1948: Progress in the statistical theory of turbulence. *Proceedings of the National Academy of Sciences of USA*, **34**, 530–539.